frontiers in Materials

ORIGINAL RESEARCH
published: 18 October 2021
doi: 10.3389/fmats.2021.754463

Effect of Cr^{6+} on the Properties of Alkali-Activated Slag Cement

Fu Bo[1,2]* *and Cheng Zhenyun*[1]

[1]College of Civil Engineering, North Minzu University, Yinchuan, China, [2]Coal Chemical Industry Technology Research Institute, National Energy Group, Ningxia Coal Industry Co., Ltd, Yinchuan, China

In order to investigate the effect of Cr^{6+} on the properties of alkali-activated slag cement (AAS), the effects of added dosage of $Na_2Cr_2O_4$ on the setting time and compressive strength of AAS were measured. The leaching concentration of Cr^{6+} from AAS cement stone was measured using dual-beam UV-visible spectrophotometry. The effect of $Na_2Cr_2O_4$ on the hydration kinetics of AAS cement was monitored by microcalorimetry and the corresponding kinetic parameters were analyzed. The pore solution from AAS was collected and analyzed using the high pressure press method. The effects of $Na_2Cr_2O_4$ on the hydration products of AAS cement were observed and compared using X-ray diffraction (XRD) and scanning electron microscopy (SEM). The experimental results showed that the AAS hydration process was markedly affected by $Na_2Cr_2O_4$ dosage. The setting time of AAS pastes was increased and the compressive strength of cement stones was reduced with increasing dosage of $Na_2Cr_2O_4$. With the development of AAS hydration, the leaching concentration of $Na_2Cr_2O_4$ gradually decreased. $Na_2Cr_2O_4$ did not affect the dissolution of slag particles, but impeded the formation of C-S-H gel. The Cr^{6+} was immobilized chemically in the form of needle-like $CaCrO_4$ particles formed by the chemical reaction between $Na_2Cr_2O_4$ and Ca^{2+} leaching from the slag.

Keywords: sodium chromate, alkaline activated slag cement, hydration behavior, hydration kinetic, hydration products

OPEN ACCESS

Edited by:
Tingting Zhang,
Dalian University of Technology, China

Reviewed by:
Linwen Yu,
Chongqing University, China
Zhuqing Yu,
Nanjing Tech University, China

***Correspondence:**
Fu Bo
20100901036@cqu.edu.cn

Specialty section:
This article was submitted to Structural Materials, a section of the journal Frontiers in Materials

Received: *06 August 2021*
Accepted: *23 September 2021*
Published: *18 October 2021*

Citation:
Bo F and Zhenyun C (2021) Effect of Cr^{6+} on the Properties of Alkali-Activated Slag Cement. Front. Mater. 8:754463. doi: 10.3389/fmats.2021.754463

INTRODUCTION

Domestic and industrial waste in urban areas are both increasing with the rapid development of China's economy. Most industrial waste contains toxic heavy metals, such as lead, chromium, copper, zinc, cadmium, nickel, etc., which exist mainly in the form of oxides, hydroxides, silicates, insoluble salts, and organic complexes. Such toxic wastes pollute the soil, water courses, and the atmosphere if not properly disposed of, which thereby results in serious environmental pollution that threatens human life and health (Liu et al., 2020).

Chromium (Cr), a typical heavy metal element, comes mainly from pigments, electroplating, metallurgy, leather tanning, Cr-containing wastewater in electronics, and from other industries. The sludge retains Cr following treatment of these Cr-containing wastewaters and of untreated and newly produced Cr residues from enterprises. Cr is toxic and can cause human respiratory and gastrointestinal diseases, as well as skin damage. In addition, Cr^{6+} is carcinogenic when inhaled into the respiratory tract, which leads to death if the amount of inhalation is large through the skin and digestive tract (I.C.D. Association, 2007).

At present, solidification technology is one of the important methods for the treatment of heavy metal lead (Pb) wastes worldwide, and cement-based materials have also been the most widely studied and applied cementing materials in developed countries in recent decades (Gougar et al., 1996; Halim et al., 2004). Research on cement-cured heavy metal Cr is quite mature, and it has been

found that cement-cured bodies have high leaching toxicity, poor durability, and poor corrosion resistance.

Alkali-activated slag cement (AAS) is a new kind of cementitious material, which is activated by alkali metal compounds from finely granulated blast furnace slag. The alkali-slag concrete derived from this process has excellent physical and mechanical properties and chemical resistance (Gougar et al., 1996; Halim et al., 2004).

AAS has an excellent pore structure, which is beneficial for reducing the leaching of Cr^{6+} into alkali-slag cement stones. AAS has a high initial strength, a stable long-term strength, and exhibits excellent mechanical sealing effects, which can comprehensively block Cr^{6+} in cement stone, thereby reducing Cr^{6+} leaching. The main product generated by the hydration of AAS is a low Ca/Si ratio C-S-H gel (Shi and Roy, 2006), which has a larger specific surface area, higher surface energy, and can strongly adsorb additional Cr^{6+}. In addition, the C-S-H gel formed by AAS hydration has a cage-like microstructure, which is more conducive to the adsorption and solidification of Cr^{6+}.

Deja (2002) studied the solidification of Cr^{6+} with slag cement and found that the nanoscale micropores in the alkali-slag gel had a great physical package effect on heavy metals. Palomo and Palacios (2003) pointed out that CrO_3 could not only solidify heavy metal ions but its addition could also improve the mechanical properties of AAS. Xu et al. (2006) studied the effect of alkali solution concentration and curing time on the solidification effect, and the results showed that the alkali concentration had little effect on the solidification effect of Cr. A large number of studies have pointed out that the effective solidification of Cr^{6+} by AAS is due to the presence of sulfides, which can convert Cr^{6+} into Cr^{3+} in a reducing environment, thereby reducing precipitation (Wang and Scrivener, 1995; Xu et al., 2006; Chen et al., 2020). Hence, AAS plays an active role in the solidification process. Zhang et al. (2016), Ponzoni et al. (2015), and Guo et al. (2017) all found that the silicate and aluminosilicate anions of the AAS system can partially chemically react with Cr^{6+} to form compounds with extremely low solubility, thus reducing the amount of Cr^{6+} leached in aqueous media.

A large number of studies have reported the solidification effect of AAS on Cr^{6+}. However, the effect of Cr^{6+} on the hydration performance of alkali-slag cement is still unclear. In this paper, the effect of $Na_2Cr_2O_4$ on the hydration process of AAS was studied under conditions where the water-binder ratio, alkali equivalent, and the modulus of the water glass were kept unchanged. First, the effect of $Na_2Cr_2O_4$ on the hydration performance of AAS was studied. Then, the effect of $Na_2Cr_2O_4$ on the hydration dynamics of AAS was investigated. Finally, the effect of $Na_2Cr_2O_4$ on the hydration products of AAS was examined.

MATERIALS AND METHODS

Raw Materials

Granulated blast furnace slag (GBFS) (Chongqing Iron and Steel Group Co., Ltd., Chongqing Municipality, China) was vibrated and ground for 40 min. This material had a specific surface area of 452 m^2/kg, a density of 2.91 g/cm^3, an alkalinity coefficient (M_0) of 1.00, an activity coefficient (M_a) of 0.45, and a mass coefficient (M_k) of 1.76. **Table 1** lists the chemical composition (main oxides) of GBFS.

NaOH (AR, Chongqing Chuanjiang Chemical Reagent Factory) was added to the purchased water glass (Chongqing Jingkou Chemical Plant; the main physical and chemical indicators are listed in **Table 2**) and its modulus adjusted to the needs of the experiment.

Tap water was used for the preparation of the solidified body, and deionized water was used for chemical analysis, including heavy metal leaching.

The chromium in $Na_2CrO_4 \cdot 4H_2O$ (AR, Chongqing Chuandong Chemical Co., Ltd.) is hexavalent, which is carcinogenic. $Na_2Cr_2O_4$ has strong oxidizing properties and is soluble in water, giving a solution that is slightly alkaline.

Table 3 lists their mix ratios (in terms of mass), the modulus of sodium silicate was fixed at 1.5, the alkali equivalent was 5%, and the water-binder ratio was 0.3. The mechanism of solidification of AAS was studied by varying the content of $Na_2Cr_2O_4$.

Methods

Slurry Curing Time Test

The determination of the curing time of AAS was carried out in accordance with the method specified in the Chinese cement standard GB/T 1346-2001 "Water consumption for standard consistency of cement, setting time, and stability test method".

Forming and Curing of the Test Block

The slag, alkali component, water, and $Na_2Cr_2O_4 \cdot 4H_2O$ were weighed out in a fixed ratio and mixed evenly in a cement slurry mixer. A 40 × 40 × 40 mm mold was used to form a solid specimen, and the molding surface was covered with a plastic film to prevent moisture evaporating. The mold was removed after 24 h at room temperature. In order to prevent the precipitation of Cr^{6+} in the specimen and the diffusion of alkali components to the condensed water on the surface of the specimen, which could lead to insufficient hardening of the surface of the cured body, the cured body specimen was placed in a sealed bag and kept in a standard indoor environment (temperature 20 ± 2°C, RH ≥ 90%) for the specified length of time.

Compressive Strength Test

The 40 × 40 × 40 mm specimens cured to 3, 7, and 28 d were removed from the standard curing room, and a universal material testing machine was employed to test the compressive strength of 3, 7, and 28 d for different cured bodies according to "Test Method for Strength of Glue Sand" (ISO Method).

Heat of Hydration Test

The heat detector of a TAM air microcalorimeter (TA Instruments, New Castle, DE, United States) was used for the heat of hydration test. The basic principle of the instrument is as follows: the heats of hydration of the sample and reference

TABLE 1 | Chemical composition of ground granulated blast furnace slag.

Chemical component	CaO	SiO_2	Al_2O_3	MgO	Fe_2O_3	Na_2O	K_2O	SO_3	MnO	Loss
wt%	36.18	32.61	14.44	9.39	1.03	0.40	0.42	0.27	0.72	0.47

TABLE 2 | Chemical composition and physical properties of water glass.

Index	SiO_2/%	Na_2O/%	Baume degree	Modulus	Density/g·cm^{-3}	Moisture content/%
Value	28.52	12.18	46	2.42	1.46	52.18

TABLE 3 | Mix proportions of alkali-activated slag cement (AAS) with $Na_2Cr_2O_4$.

No.	Water/ cement	Na_2O (%)	Modulus of water glass	$Na_2Cr_2O_4$ content (%)
1	0.30	5.0	1.5	0.0
2				0.5
3				1.0
4				1.5
5				2.0

sample are measured using a thermocouple (water or the completely hydrated cement stone is usually selected as the reference sample) in a constant temperature environment, and the exothermic rate and cumulative heat release of the sample are calculated. The test temperature was set at 20°C. Measurements were carried out on 4 g samples of the pastes. The solution of $Na_2Cr_2O_4$ was added in the proportions given in **Table 3**. Heat development was measured for 72 h, with a step of 50 s between consecutive measurements. Before the experiment, slag was placed in an ampoule, the solution was placed in a syringe, and the ampoule was placed in the calorimeter. After the syringe had been installed, the solution was injected into the ampoule when the temperature had stabilized at 20°C, when measurement began.

Heavy Metal Concentration Measurement

According to the national standards GB 5086.1-1997 "Solid Waste Leaching Toxicity Leaching Method Reversal Method" and GB/T 15,555.4-1995 "Solid Waste Determination of Hexavalent Chromium Diphenylcarbazide Spectrophotometer Method," the molded test piece was broken and a sample passing through a 5 mm sieve was placed in an oven and dried at 60°C, and then soaked in deionized water at a liquid-to-solid ratio (L/g) of 1:10. Subsequently, the mixture was vibrated at 23 ± 2°C for 18 h with a flip-type shaking device at a speed of 30 ± 2 rev/min, and kept for 30 min, and then the leaching solution was collected with a vacuum filter. A dual-beam UV-Vis spectrophotometer TU-190 made by Beijing General Instrument Co. Ltd. was used to measure the concentration of Cr^{6+} in the leaching solution.

Testing of Block Hole Solution

The alkali-slag-Cr^{6+} solidified body pore solution extrusion test piece was prepared using a special molding test mold (Jiangsu Subote Materials Co., Ltd., Nanjing, Jiangsu, China). The test piece was sealed in a plastic bag and then placed in standard storage environment (temperature: 20 ± 2°C; RH ≥ 90%) for the specified time. The hole solution pressing device of cement-based material was then used to squeeze the hole solution, and the dual-beam spectrophotometer was used to test the Cr^{6+} concentration in the hole solution.

X-Ray Diffraction Test

The sample was broken following curing for the specified time and hydration was immediately terminated using absolute ethanol. The sample was then baked to a constant weight at 60°C and passed through a 0.08 mm sieve. The powder was then sealed in an ampoule for later testing.

A Rigaku D/Max-5A 12 kW rotating target X-ray diffractometer (Rigaku Corporation, Tokyo, Japan) was used for testing, with Cu Kα radiation at a voltage of 40 kV and a scanning speed of 4°/min. The sample was dried to constant weight in a vacuum drying oven at 60°C before the test.

Scanning Electron Microscope Test

The sample was broken following curing for the specified time and hydration was immediately terminated with absolute ethanol. The sample was then baked to a constant weight at 60°C and sprayed with gold on a cross-section for later testing.

A variable vacuum scanning electron microscope (TESCAN VEGA2, Tescan Brno, s.r.o, Brno, Czech Republic) was adopted for morphological characterization, and an INCA Energy 350X energy dispersive X-ray spectrometer (Oxford Instruments, Oxford, United Kingdom) was employed for elemental analysis.

RESULTS AND DISCUSSION

Macroscopic Performance of $Na_2Cr_2O_4$-AAS

Variation in Curing Time

Figure 1 shows the effect of $Na_2Cr_2O_4$ on the curing time of AAS. It can be seen that the latter gradually increased as the $Na_2Cr_2O_4$ content increased. The initial setting time of AAS

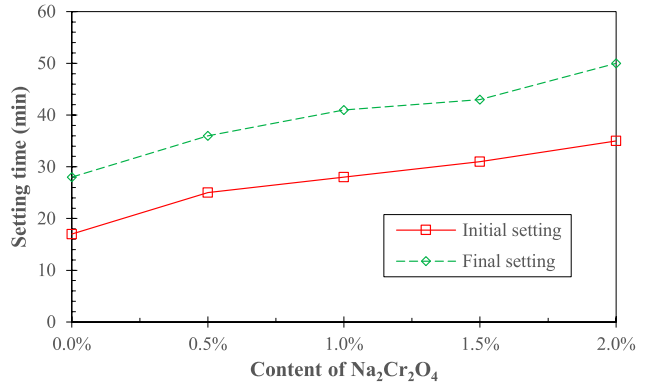

FIGURE 1 | Setting time of alkali-activated slag cement (AAS).

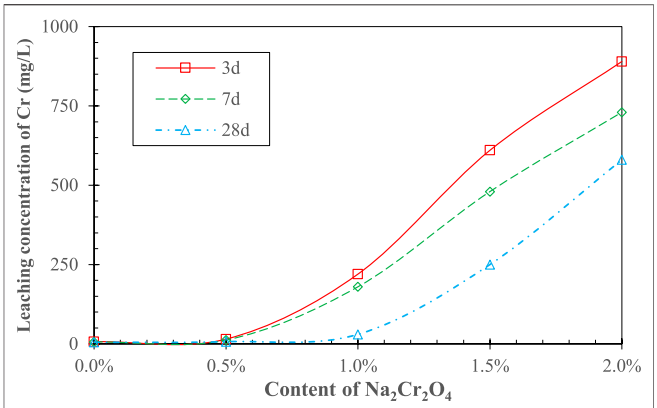

FIGURE 3 | Concentration of Cr^{6+} leaching from AAS.

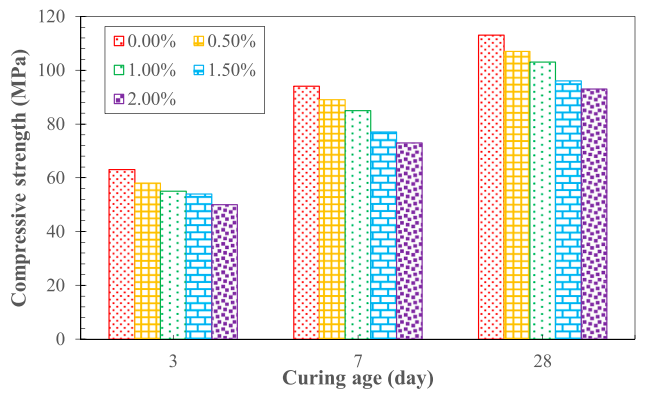

FIGURE 2 | Compressive strength of AAS.

with 2% $Na_2Cr_2O_4$ increased from 17 to 35 min, compared with that of the control AAS, and the final curing time increased from 28 to 50 min, both of which were doubled. This is consistent with the results of previous studies (Palomo and Palacios, 2003).

Variation in Compressive Strength

Figure 2 shows the effect of $Na_2Cr_2O_4$ on the compressive strength of AAS. It can be seen that the latter decreased with increasing concentration of $Na_2Cr_2O_4$ for the same curing age. The compressive strength of cement with different $Na_2Cr_2O_4$ content increased with age.

The curing time and strength development of AAS are two important macro indicators that reflect the hydration process (Shi and Roy, 2006; Pacheco-Torgal et al., 2015). As shown in **Figures 1**, **2**, the addition of $Na_2Cr_2O_4$ played a significant role in the hydration process of AAS, and the effect increased with increasing concentration of $Na_2Cr_2O_4$. Fang et al. (2020) pointed out that when the chemical substances introduced into the AAS hydration system combine with the Ca^{2+} ions or $[SiO_4]^{4-}$ ions generated by the disintegration of the slag and OH^- ions in the system under the action of the alkali component, forming small-sized particles of insoluble substances, they may form precipitates on the surface of the slag particles, hindering further hydration reactions with OH^- ions and activating components.

Leaching Concentration of Cr^{6+}

Figure 3 shows the concentration of Cr^{6+} leaching from the AAS stone. It can be seen that at both 3 and 7 d, Cr^{6+} was effectively solidified in the AAS when the $Na_2Cr_2O_4$ content was less than 0.5%. The concentration of Cr^{6+} leaching out increased significantly when the $Na_2Cr_2O_4$ content was greater than 0.5%, and it rose sharply with increasing amounts of $Na_2Cr_2O_4$. Therefore, it can be conjectured that the initial leaching concentration of Cr^{6+} has a critical value when the concentration of $Na_2Cr_2O_4$ is 0.5% for this cement mix. In addition, the Cr^{6+} leaching concentration for AAS stone at 28 d also appeared to follow a similar pattern, whereas the Na_2Cr_2O4 content for a critical leaching concentration increased from 0.5 to ~1.0%.

From the previous analysis, it can be seen that the introduction of $Na_2Cr_2O_4$ led to a low degree of initial hydration of AAS, so that the porosity of the initial cement stone and the leaching rate of Cr^{6+} are both increased, leading to a low leaching concentration threshold. The density of the AAS stone gradually increased, and the porosity gradually decreased with increasing age, so that the leaching rate of Cr^{6+} was small, and the $Na_2Cr_2O_4$ content for a critical leaching concentration increased with extension of the hydration time.

Hydration Exothermic Behavior of $Na_2Cr_2O_4$-AAS

From the previous analysis, it can be seen that the solidification of Cr^{6+} is closely related to the hydration process of AAS. In order to further study the solidification mechanism of AAS on Cr^{6+}, the effect of $Na_2Cr_2O_4$ on the hydration exothermic process of AAS was studied (**Figure 4**).

Figure 4A shows the exothermic hydration rate of AAS for the $Na_2Cr_2O_4$ group and the control group, among which the control group was AAS without Cr^{6+}. In the $Na_2Cr_2O_4$ group, the $Na_2Cr_2O_4$ content was 1.0%, and the content of the rest of the material was the same as that of the control group. The figure

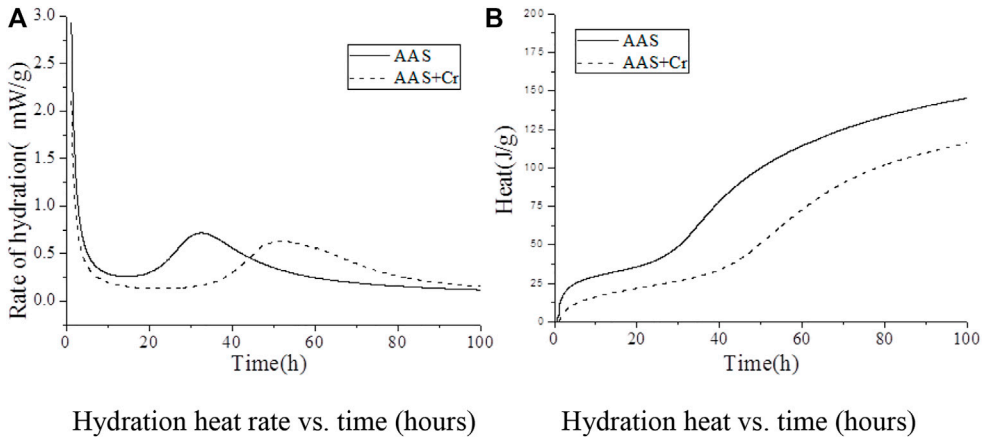

FIGURE 4 | Isothermal calorimetric analysis of AAS: **(A)** rate of hydration as a function of time; **(B)** cumulative heat of hydration.

shows that, compared with the control group, the AAS exothermic hydration rate of the $Na_2Cr_2O_4$ group was significantly prolonged.

Figure 4B shows the total hydration heat released by AAS in the $Na_2Cr_2O_4$ group and the control group. It can be seen that the AAS hydration of the $Na_2Cr_2O_4$ group was always significantly lower than that of the control group and that the variation in the total hydration heat released by the two groups were completely different. It can be seen from **Figure 4A** that there is an obvious exothermic peak in the early stages for the two groups, which was caused by the destruction of the slag surface by OH^- ions and the formation of C-S-H gel on the surface of the slag particles (Shi and Roy, 2006). However, it can be seen from the total quantity of heat released during the corresponding time in **Figure 4B** that the total quantity of heat released in the $Na_2Cr_2O_4$ group during this time was significantly lower than that of the control group. It is inferred that $Na_2Cr_2O_4$ prevents OH^- ions from destroying the slag structure or forming C-S-H gel on the slag surface. The $Na_2Cr_2O_4$ group showed a longer induction period (**Figure 4A**), and the total quantity of corresponding hydration heat released was much lower than that of the control group (**Figure 4B**). It can be inferred that $Na_2Cr_2O_4$ chemically reacts with the ions in the liquid phase to form insoluble substances on the surface of the slag particles, which prevents Ca^{2+} ions from reacting with SiO_4^{4-} in the liquid phase to form C-S-H gel. After entering the acceleration period, the variation in heat released for the two groups was identical, although the heat released by the $Na_2Cr_2O_4$ group was always lower than that of the control group. The effect of $Na_2Cr_2O_4$ on the hydration process of AAS was therefore weakened. In summary, the introduction of $Na_2Cr_2O_4$ significantly changed the hydration process of AAS according to Hess's law (Gersten and Gersten, 2001). In order to further understand the effect of $Na_2Cr_2O_4$ on the hydration process of AAS, the corresponding hydration kinetic parameters were calculated from the hydration heat release curve of the alkali-slag cement, the Knudson hydration heat model, and the Jander equation (**Table 4**).

TABLE 4 | Hydration kinetic parameters of AAS.

Hydration process	—	AAS	AAS +1% Cr6+
Acceleration stage	Time	15.80–32.5	38.44–54.35
	N	1.95	1.36
	K	1.71×10^{-3}	3.21×10^{-3}
Deceleration stage	Time	32.53–59.4	54.35–89.18
	N	2.01	1.37
	K	2.51×10^{-3}	3.37×10^{-3}
Attenuation stage	Time	59.43–100	89.18–100
	N	2.22	2.01
	K	1.17×10^{-4}	1.12×10^{-4}

Table 4 lists the AAS hydration kinetic parameters of the $Na_2Cr_2O_4$ group and the control group. It can be seen from the data listed in the table that the start time of the acceleration period in the $Na_2Cr_2O_4$ group was about 2.4 times that of the control group, and the start time of the deceleration period was about 1.7 times that of the control group. $Na_2Cr_2O_4$ significantly prolonged the curing time of AAS. In **Table 4**, N represents the order of the chemical reaction, which mainly characterizes the degree of difficulty of the reaction. The latter is controlled by chemical reactions on the particle surfaces and by the dissolution of reactants or the deposition of reaction products when $N \leq 1$. The reaction is controlled by the diffusion of reactants through the porous reaction product layer when $1 \leq N \leq 2$. The reaction is controlled by the diffusion of reactants through the dense product layer when $2 \leq N$ (Shi and Roy, 2006). K represents the rate constant of the chemical reaction, which characterizes the speed of the chemical reaction (Gersten and Gersten, 2001).

It can be seen from **Table 4** that the reaction rate of AAS in the $Na_2Cr_2O_4$ group during both the acceleration and deceleration periods was significantly higher than that of the control group, yet the reaction order was significantly lower than that of the control group. According to the AAS hydration process (Zhang et al., 2016), the chemical reaction order N of the whole hydration process was around 2 for the control group,

TABLE 5 | Pore solution obtained from solidification of AAS-Cr^{6+} (mg/L).

Age/kind	1 d			3 d			7 d		
	Total Cr	Cr^{6+}	Ca^{2+}	Total Cr	Cr^{6+}	Ca^{2+}	Total Cr	Cr^{6+}	Ca^{2+}
AAS	2.267	2.035	1.64	2.253	2.241	0.85	2.357	2.301	0.475
AAS + Cr	9635.58	7,125.65	2.3	7,056.616	6,023.65	1.4	6,245.069	4,952.26	0.775

indicating that the hydration process of the control group was more prone to being controlled by the diffusion of reactants through the dense product layer from the acceleration period. The main hydration products of sodium silicate activated in AAS were mainly low calcium-to-silicon ratio C-S-H gel, which has low porosity and a compact structure (Shi and Roy, 2006). Although the reaction rate of Ca^{2+} and SiO_4^{4-} was rapid in the liquid phase, it is not easy for Ca^{2+} to penetrate the hydration product layer and enter the liquid phase in order to react. For the $Na_2Cr_2O_4$ group, the reaction order *N* was closer to 1, although the reaction rate was faster during both the acceleration and deceleration periods, indicating that the hydration process was more prone to being controlled by the diffusion of reactants through the porous reaction product layer from the acceleration period. Based on this, it can be further speculated that $Na_2Cr_2O_4$ first forms a poorly soluble porous product on the surface of the slag particles with the substance in the liquid phase. After entering the decay period, the reaction rate constants and reaction orders of the two groups were equivalent, and both were controlled by the diffusion of the reactants through the dense product layer, at which time C-S-H gel should have been generated.

Pore Solution and Hydration Products of $Na_2Cr_2O_4$-AAS

Analysis of Pore Solution of AAS

In this study, a cement-based material pore solution pressing device (Jiangsu Subote Materials Co., Ltd.) was used to collect different cement paste and pore solutions of the paste solidification body. The solidification effect of AAS on heavy metal Cr^{6+} ions during the hydration process was investigated by analyzing the ion concentration of the pore solution and using the analysis of hydration kinetics described above.

Table 5 shows that the total Cr, Cr^{6+}, and Ca^{2+} concentrations in the liquid phase gradually decreased with the progress of hydration. The Ca^{2+} concentration of the pore solution in the AAS stone depended mainly on the degree of disintegration of the slag glass body and the amount of C-S-H gel hydration product. With the extension of hydration time, OH^- ions were continuously consumed, and the formation of hydration products gradually increased. The hydration product layer gradually changed from a porous structure to a dense structure, which reduced the amount available for disintegration of the slag glass structure as well as the concentration of Ca^{2+}. The concentrations of total Cr and Cr^{6+} in the alkali-slag solidified body were reduced as a function of time due to the reduction of Cr^{6+} by S^{2-} or HS^- in the slag and the enhanced adsorption of Cr^{6+} by the hydration products.

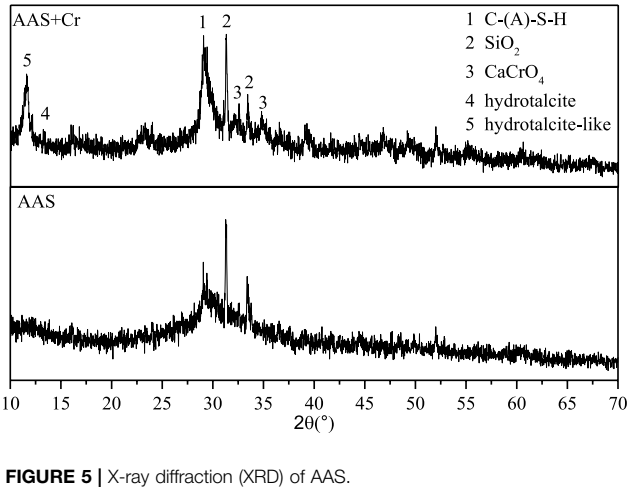

FIGURE 5 | X-ray diffraction (XRD) of AAS.

At 1 d, the Ca^{2+} content in the AAS pore solution of the $Na_2Cr_2O_4$ group was significantly higher than that of the control group. This shows that $Na_2Cr_2O_4$ can promote the dissolution of slag particles. At 3 and 7 d, the Ca^{2+} content in the AAS pore solution of the $Na_2Cr_2O_4$ group was higher than that of the control group. The heat of hydration experiment showed that the rates of hydration of the $Na_2Cr_2O_4$ group in the initial age were lower than those of the control group, indicating that $Na_2Cr_2O_4$ delayed the Ca^{2+}, which dissolved from the slag, from reacting with SiO_4^{4-} in the liquid phase to form C-S-H gel, which led to a delay in the second hydration reaction peak in the heat of hydration experiment.

Hydration Products of AAS

Figure 5 shows the XRD pattern of AAS stone at 28 d. It can be seen that a typical "Bailey broad peak" appeared around 30°, which originated from the C-S-H gel. There are two obvious peaks at 32.3° and 35.2°, both originating from $CaCrO_4$ (Wang and Vipulanandan, 2000; Chen et al., 2009). Combined with the analysis of the hydration kinetic process, it can be known that $Na_2Cr_2O_4$ hydrolyzes to form CrO_4^{2-}, which reacts with the dissolved Ca^{2+} in the slag to form $CaCrO_4$, hence preventing Ca^{2+} from interacting with SiO_4^{4-} in the liquid phase to generate C-S-H gel. This reduces the strength of AAS.

Figure 6 shows the SEM images of AAS stones in both the $Na_2Cr_2O_4$ group and control groups at 28 d. It can be seen from the control group that the slag was basically hydrated, forming a continuous dense structure with fewer pores. In addition, it can be seen from the $Na_2Cr_2O_4$ group that the structure of the

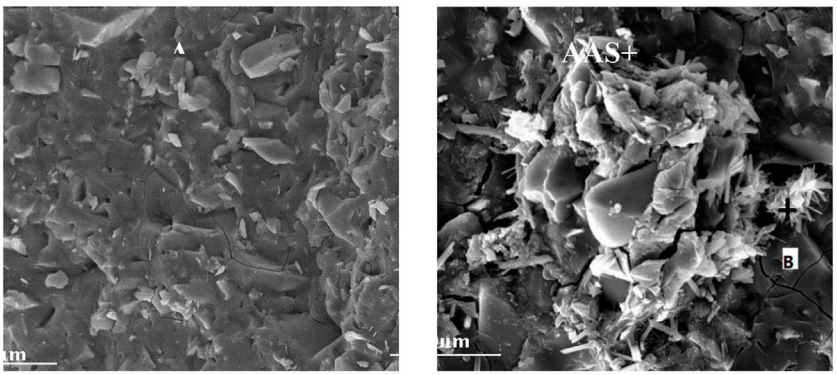

FIGURE 6 | Scanning electron micrograph (SEM) of AAS-Cr^{6+} solidification.

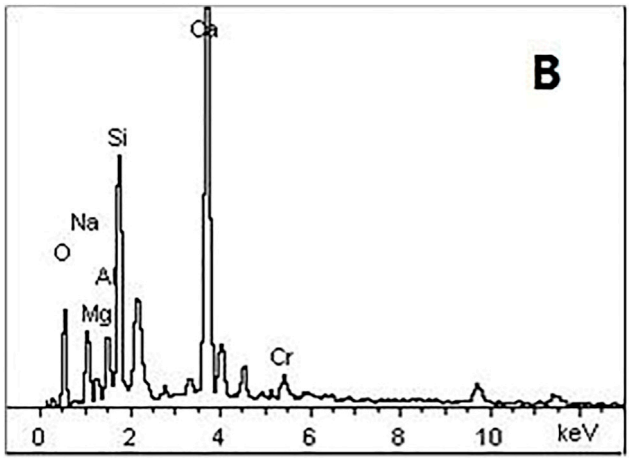

FIGURE 7 | Energy dispersive spectrum (EDS) of AAS-Cr^{6+} solidification.

hydration products was relatively loose, and needles and rods were formed. The needles and rods (point B) were analyzed using energy dispersive spectroscopy (EDS) (**Figure 7**). The results showed that the weight percentage of elemental Cr at this point was 3.23%, which was much higher than the original amount in the mix (1%). In addition, a large amount of Ca was enriched here. According to the results of Laforest and Duchesne (2005), the rod-shaped crystals here were $CaCrO_4$.

CONCLUSION

The curing time of AAS in our experiments was prolonged and the strength of the cement stone gradually decreased with increasing $Na_2Cr_2O_4$ content. The leaching of $Na_2Cr_2O_4$ gradually decreased with increasing hydration age. At this AAS mix ratio, the leaching limit value of $Na_2Cr_2O_4$ at 3 and 7 d was 0.5% and at 28 d was 1.0%. $Na_2Cr_2O_4$ did not affect the way OH^- ions destroyed the slag structure, but mainly affected the reaction of Ca^{2+} ions dissolved in the slag with SiO_4^{4-} ions in the liquid phase to form C-S-H gel. $Na_2Cr_2O_4$ and Ca^{2+} precipitated in the slag to form rod-shaped $CaCrO_4$ particles, which chemically solidified Cr^{6+}.

DATA AVAILABILITY STATEMENT

The original contributions presented in the study are included in the article/Supplementary Material, further inquiries can be directed to the corresponding author.

AUTHOR CONTRIBUTIONS

FB investigated the data and wrote the manuscript. CZ designed the experiments and was involved in data analysis.

FUNDING

This study was financially supported by 2019 Key Research Project of North Minzu University (2019KJ31). The support of the National Natural Science Foundation of China (Grant No. 51668001), the Key Research and Development Program of Ningxia Hui Autonomous Region (2020BDE03009) and the Natural Science Foundation of Ningxia Hui Autonomous Region (2020AAC03195; 2021AAC03187) is also gratefully acknowledged.

REFERENCES

I.C.D. Association (2007). *Health Safety and Environment Guidelines for Chromium, Revision*.

Chen, H., Yuan, H., Mao, L., Hashmi, M. Z., Xu, F., and Tang, X. (2020). Stabilization/solidification of Chromium-Bearing Electroplating Sludge with Alkali-Activated Slag Binders. *Chemosphere* 240, 124885. doi:10.1016/j.chemosphere.2019.124885

Chen, Q. Y., Tyrer, M., Hills, C. D., Yang, X. M., and Carey, P. (2009). Cheminform Abstract: Immobilization of Heavy Metal in Cement-Based Solidification/

stabilisation: A Review. *ChemInform* 40 (23), 390–403. doi:10.1002/chin.200923207

Deja, J. (2002). Immobilization of Cr6+, Cd2+, Zn2+ and Pb2+ in Alkali-Activated Slag Binders. *Cement Concrete Res.* 32, 1971–1979. doi:10.1016/S0008-8846(02)00904-3

Fang, S., Lam, E. S. S., Li, B., and Wu, B. (2020). Effect of Alkali Contents, Moduli and Curing Time on Engineering Properties of Alkali Activated Slag. *Construction Building Mater.* 249 (6), 118799. doi:10.1016/j.conbuildmat.2020.118799

Gougar, M. L. D., Scheetz, B. E., and Roy, D. M. (1996). Ettringite and C-S-H Portland Cement Phases for Waste Ion Immobilization: A Review. *Waste Management* 16 (4), 295–303. doi:10.1016/S0956-053X(96)00072-4

Guo, X., Zhang, L., Huang, J., and Shi, H. (2017). Detoxification and Solidification of Heavy Metal of Chromium Using Fly Ash-Based Geopolymer with Chemical Agents. *Construction Building Mater.* 151, 394–404. doi:10.1016/j.conbuildmat.2017.05.199

Halim, C. E., Amal, R., Beydoun, D., Scott, J. A., and Low, G. (2004). Implications of the Structure of Cementitious Wastes Containing Pb(II), Cd(II), As(V), and Cr(VI) on the Leaching of Metals. *Cement Concrete Res.* 34, 1093–1102. doi:10.1016/j.cemconres.2003.11.025

Laforest, G., and Duchesne, J. (2005). Immobilization of Chromium (VI) Evaluated by Binding Isotherms for Ground Granulated Blast Furnace Slag and Ordinary Portland Cement. *Cement Concrete Res.* 35 (12), 2322–2332. doi:10.1016/j.cemconres.2004.12.011

Liu, M., Li, X., He, Y., and Li, H. (2020). Aquatic Toxicity of Heavy Metal-Containing Wastewater Effluent Treated Using Vertical Flow Constructed Wetlands. *Sci. Total Environ.* 727, 138616. doi:10.1016/j.scitotenv.2020.138616

Pacheco-Torgal, F., Labrincha, J. A., Leonelli, C., Palomo, A., and Chindaprasirt, P. (2015). *Handbook of Alkali-Activated Cements, Mortars and Concretes*. Cambridge: Woodhead Publishing. doi:10.1016/C2013-0-16511-7

Palomo, A., and Palacios, M. (2003). Alkali-activated Cementitious Materials: Alternative Matrices for the Immobilisation of Hazardous Wastes. *Cement Concrete Res.* 33 (2), 289–295. doi:10.1016/s0008-8846(02)00964-x

Ponzoni, C., Lancellotti, I., Barbieri, L., Spinella, A., Saladino, M. L., and Martino, D. C. (2015). Chromium Liquid Waste Inertization in an Inorganic Alkali Activated Matrix: Leaching and NMR Multinuclear Approach. *J. Hazard. Mater.* 286, 474–483. doi:10.1016/j.jhazmat.2014.12.054

Gersten, J. I., and Gersten, J. I. (2002). *The Physics and Chemistry of Materials*, 55. New York: John Wiley & Sons, 59–60. doi:10.1063/1.1506755

Shi, C., and Roy, D. (2006). *Alkali-Activated Cements and Concretes*. Boca Raton: CRC Press.

Wang, S. D., and Scrivener, K. L. (1995). Hydration Products of Alkali Activated Slag Cement. *Cement Concrete Res.* 25 (3), 561–571. doi:10.1016/0008-8846(95)00045-E

Wang, S., and Vipulanandan, C. (2000). Solidification/stabilization of Cr(VI) with Cement: Leachability and XRD Analyses. *Cement Concrete Res.* 30, 385–389. doi:10.1016/S0008-8846(99)00265-3

Xu, J. Z., Zhou, Y. L., Chang, Q., and Qu, H. Q. (2006). Study on the Factors of Affecting the Immobilization of Heavy Metals in Fly Ash-Based Geopolymers. *Mater. Lett.* 60 (6), 820–822. doi:10.1016/j.matlet.2005.10.019

Zhang, W., Yang, C., Yang, K., and Pan, Q. (2016). Effect of Sal Perlatum-Water Glass on the Hydratioin Behavior of Alkali-Activated Slag Cements. *J. Building Mater.* 19, 803–809. doi:10.3969/j.issn.1007-9629.2016.05.003

Conflict of Interest: FB was employed by the company Coal Chemical Industry Technology Research Institute, National Energy Group, Ningxia Coal Industry Co., Ltd.

The remaining author declare that the research was conducted in the absence of any commercial or financial relationships that could be construed as a potential conflict of interest.

Publisher's Note: All claims expressed in this article are solely those of the authors and do not necessarily represent those of their affiliated organizations, or those of the publisher, the editors and the reviewers. Any product that may be evaluated in this article, or claim that may be made by its manufacturer, is not guaranteed or endorsed by the publisher.